High Temperature Tribological Properties of Al₂O₃/NCD Films Investigated Under Ambient Air Conditions

Vitali Podgursky [1],* , **Maxim Yashin [1]** , **Taivo Jõgiaas [2]** , **Mart Viljus [1]** , **Asad Alamgir [1]** ,
Mati Danilson [3] and **Andrei Bogatov [1]**

[1] Department of Mechanical and Industrial Engineering, Tallinn University of Technology, Ehitajate tee 5,
    19086 Tallinn, Estonia; mayash@taltech.ee (M.Y.); mart.viljus@taltech.ee (M.V.);
    asad.shaikh@taltech.ee (A.A.); andrei.bogatov@mail.ru (A.B.)

[2] Institute of Physics, University of Tartu, W. Ostwaldi 1, 50411 Tartu, Estonia; taivo.jogiaas@ut.ee

[3] Department of Materials and Environmental Technology, Tallinn University of Technology, Ehitajate tee 5,
    19086 Tallinn, Estonia; mati.danilson@taltech.ee

* Correspondence: vitali.podgurski@taltech.ee; Tel.: +372-6203-358

Abstract: Comparative analysis of dry sliding wear behavior of nanocrystalline diamond (NCD) films and NCD films coated with a thin Al₂O₃ layer (Al₂O₃/NCD) is the main goal of the present study. Plasma-enhanced chemical vapor deposition (PECVD) and atomic layer deposition (ALD) methods were used to prepare the NCD and alumina films, respectively. Sliding wear tests were conducted at room temperature (RT), 300 and 450 °C in air. Independent of type of specimen, superlubricating behavior with the coefficient of friction (COF) in the range of 0.004-0.04 was found for the tests at 300 °C. However, the COF value measured on the Al₂O₃/NCD films in the tests at 450 °C is lower than that for the NCD film. A relatively short run-in period and a stable COF value of about 0.15 were observed at this temperature for the Al₂O₃/NCD films. The width of the wear scars measured on the Al₂O₃/NCD films after the tests at 450 °C is significantly smaller in comparison with the NCD film. The apparent wear volume of the wear scar on the NCD film tested at 450 °C was noticeably higher than that on the Al₂O₃/NCD films.

Keywords: diamond films; oxidation; tribology; high temperature

1. Introduction

Diamond is important engineering material due to outstanding properties including high Young's modulus, hardness and low coefficient of friction (COF). The fundamental drawback of carbon-based coatings (diamond like carbon and different types of diamond coatings) used in industry is the oxidation at high temperatures under ambient conditions, which strongly reduces the applicability of these materials at elevated temperatures. The thermal stability of carbon-based materials depends on the crystal structure. Diamond oxidation starts at >450 °C in open air, i.e., in the presence of water and oxygen [1,2]. In the case of nanocrystalline diamond (NCD) films, the oxidation begins at the grain boundaries followed by oxidation of diamond grains [3].

The tribological behavior of diamond coatings at high temperatures in ambient air has been studied in the past. Erdemir and Fenske [4] investigated friction and wear of the NCD films prepared on SiC in sliding tests against SiC pins at temperatures up to 400 °C. The initial COF value was between 0.6-0.7. It was found that the COF value for the steady-state period of sliding increases from 0.25 in the test at 300 °C to 0.5 in one at 400 °C, as well as a significant increase of the wear rate of the SiC pins was observed at 400 °C. The tribological properties of the NCD film at high temperatures were investigated

by Yashin et al. [5]; the Si_3N_4 balls were used as a counterbody. The COF value for the early period of run-in was between 0.6-0.8 independent of the temperature of the test; however, the duration of this period of sliding with high COF increased with the increase of temperature. In the case of the steady state period of sliding, the COF value varied, i.e., it was 0.13, 0.3 and 0.4 for tests at room temperature (RT), 300 and 450 °C, respectively. The significant increase of the wear scar width on the films was observed after the test at 450 °C in comparison with the tests at RT and 300 °C.

The improvement of tribological properties of carbon materials at elevated temperatures is a technological challenge. Different approaches were used to improve the thermal stability and tribological properties of the Diamond-like carbon (DLC) coatings at high temperature. Relatively low COF and wear rate were found on the W-doped DLC in the sliding tests up to 500 °C; these properties were attributed to the formation of a tungsten oxide layer on the coating surface [6]. Oxygen plasma treatment of Si-doped DLC coating surface improved the thermal stability of DLC, due to the formation of an SiO_2 layer [7]. In another approach, the Si-doped DLC coating was annealed at 500 °C for 30 min in ambient air, to prepare an SiO_2 oxide layer on top of DLC, and the good tribological properties were demonstrated at 400 °C [8]. Recently, it was shown that doping of diamond with boron leads to the formation of a B_2O_3 oxide layer on a diamond surface, resulting in improvement of the oxidation resistance of diamond [2]. The Al_2O_3 was deposited by atomic layer deposition (ALD) on diamond particles and an improvement of oxidation resistance was demonstrated [9]. The deposition of the Al_2O_3 layer by ALD on the diamond surface was carried out to prepare a gate insulator for diamond field effect transistor (FET). The Al_2O_3 film on diamond shows stoichiometric composition, abrupt interface between Al_2O_3 and diamond, and can be deposited conformal [10]. Therefore, a promising direction for further research is the investigation of diamond coatings coated with an oxide layer, which can play a decisive role in the improvement of tribological properties at high temperature in the air. Alumina (Al_2O_3) has many advantageous properties including high thermal and chemical stability, high hardness at elevated temperatures, and low solubility in many work materials [11].

The main goal of the present study is the investigation of the tribological properties of the NCD and Al_2O_3/NCD films. The study focuses on the protection of the diamond films against oxidation attack at high temperature in ambient atmosphere and, simultaneously, on the preservation of the excellent tribological properties of the NCD films. A relatively thin alumina layer was used as an effective protection layer against the oxidation of the NCD films. It is taken into account in advance that due to high contact pressure between the counterbodies, the thin oxide layer must be broken down within the contact between the counterbodies already at the beginning of the sliding test. Therefore, a contact between the NCD film surface and the ball can be established and excellent lubrication conditions can be achieved.

Due to small thickness of the Al_2O_3 layer, the correct selection of the characterization methods is important. The X-ray diffractometer in grazing incidence mode was used to analyze the crystal structure of the Al_2O_3 layer, and X-ray photoelectron spectroscopy (XPS) was used for measurement of the elemental composition and chemical and electronic states of the elements within the ultrathin surface layers.

2. Materials and Methods

The 3-μm-thick NCD film was grown on an (100)-oriented Si wafer by microwave plasma enhanced chemical vapor deposition (MW-PECVD). The Si wafer was manually scratched by diamond powder prior to deposition; the powder particles size was 0.5-1 μm. The synthesis of diamond films was carried out in a MW-PECVD system UPSA-100 (2.45 GHz, 5 kW) using a CH_4/H_2/air plasma. The substrate temperature was 900 °C, total flow rate 500 sccm, pressure 45 Torr, microwave power 2.5 kW, volume fraction of methane 20%, and air 0.3%. After deposition of the NCD film, the wafer was mechanically cut into rectangular pieces of equal size, in total nine pieces 8 × 8 mm in size were prepared.

Atomic layer deposition (ALD) method was used to prepare Al_2O_3 films. Six samples were coated with an alumina layer. The deposition was conducted in flow-type reactor Picosun R200 at 300 °C

using trimethylaluminum (TMA) and water as precursors and nitrogen (5.0 purity) as purge gas. The pressure was 10 mbar. The precursor pulse lengths were 0.1, 4, 0.1, and 10 s for TMA, N_2, H_2O, and N_2, respectively. After 2000 cycles, the thickness of Al_2O_3 films was 220 nm. Spectroscopic ellipsometer (SemilabSopraGES-5E, Semilab, Budapest, Hungary) was used to measure the film thickness, using 365 and 633 nm wavelengths at an angle of 75° on Si (100) reference substrates. The fitting was performed using Cauchy approximation. Three samples (A-Al_2O_3/NCD) were further annealed in ambient air at 500 °C during 3 h.

Ball-on-disk type of tribometer, equipped with a high-temperature chamber with rotary drive was used for investigation of the tribological behavior of the specimens. The Ø 10 mm Si_3N_4 balls were used as a counterbody. Wear tests at RT, 300 and 450 °C were carried out on each type of specimen, i.e., uncoated NCD, as-deposited Al_2O_3/NCD and annealed A-Al_2O_3/NCD films. Normal load was 3 N, rotation speed 300 rpm, and tests duration 3 h. The sliding track diameter was 3 mm.

Depth, width and shape of wear scars were investigated using stylus profilometry (Mahr Perthometer). Five line scans were taken across each wear scar, and the averaged line scan was obtained. Apparent volume (V) of the wear scar was estimated using formula $V = S \times l$, where the cross-section area is S, and the wear scar length is l.

X-ray diffraction (XRD), Micro-Raman spectroscopy, X-ray photoelectron spectroscopy (XPS), and Scanning electron microscopy (SEM) were used to evaluate the chemical structure and to monitor the morphology of the pristine and wear scars surfaces. The structure and phase compositions were determined using Rigaku Smartlab X-ray diffractometer in grazing incidence mode with the incidence omega angle of 0.5°. Copper k-alpha wavelength of 1.540598 Å and 2 theta scan range of 15°–100° were used. The micro-Raman measurements were carried out on a Renishaw inVia micro-Raman (Renishaw, New Milles, UK) setup equipped with an Ar+ ion laser (514 nm wavelength). The information on the composition was studied using XPS in a Kratos Analytical AXIS ULTRA DLD (Kratos Analytical Ltd., Manchester, UK) spectrometer fitted with a monochromatic Al K_α X-rays source and achromatic Mg K_α/Al K_α dual anode X-ray source. A monochromatic Al K_α anode (1486.6 eV) was used, operated at 150 W and 15 kV. The 180° hemispherical energy analyzer with 165 mm mean radius was operated using a hybrid lens mode at pass energy 160 eV for survey spectra, 20 eV for regions and 40 eV for regions acquired for depth profile. XPS spectra were recorded at 90° takeoff angle from the surface of the sample holder using an aperture field of view Ø 220 μm. Samples were mounted on a stainless steel 130×15 mm^2 sample bar. Binding energy values were calculated on the basis of the C 1s peak at 284.6 eV. For surface cleaning and bulk composition information, Minibeam I ion (Ar^+) source (1 kV, 10 mA, 120 s per cycle) was used. The SEM images were taken by the Zeiss EVO®® MA - 15 system with LaB6 cathode in secondary electron mode, applying an accelerating voltage of 10–15 kV and 6.5–8.5 mm working distance.

3. Results and Discussion

Figure 1 shows SEM images taken on the NCD and Al_2O_3/NCD films. The XRD pattern taken in grazing incident mode from the as-deposited Al_2O_3/NCD film is shown in Figure 2. The peak positions are similar to the reflections from the NCD film investigated in our previous study of the NCD films grown on Si(100) and (110) single crystal diamond [12,13]; no peaks corresponding to Si and β-SiC were observed due to grazing incident set-up. The Al_2O_3 layer prepared at low temperature is amorphous [14–16]. The conformal growth of the Al_2O_3 islands with globular shape was observed on the NCD film in agreement with Ref. [10].

(a)

(b)
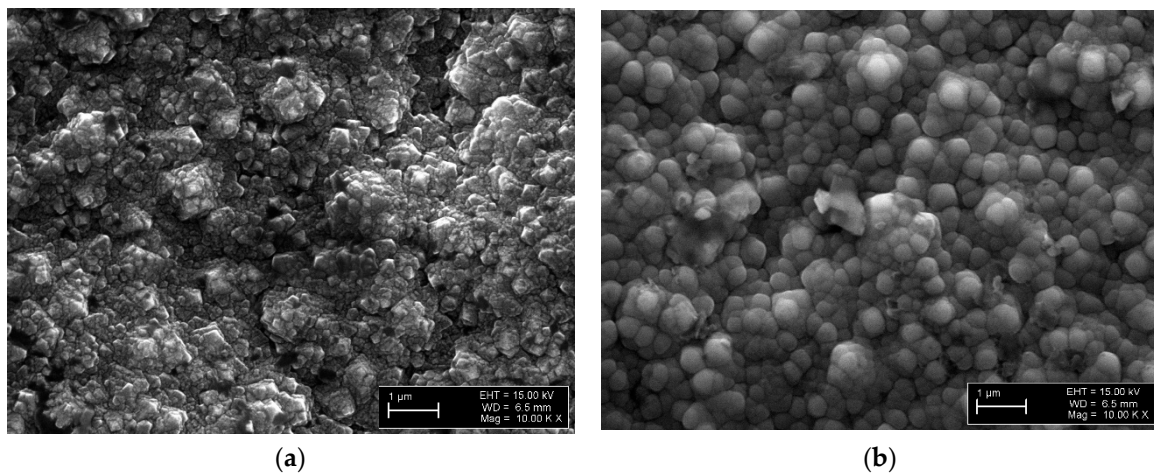
Figure 1. (**a**) SEM images of the NCD and (**b**) Al_2O_3 /NCD films.
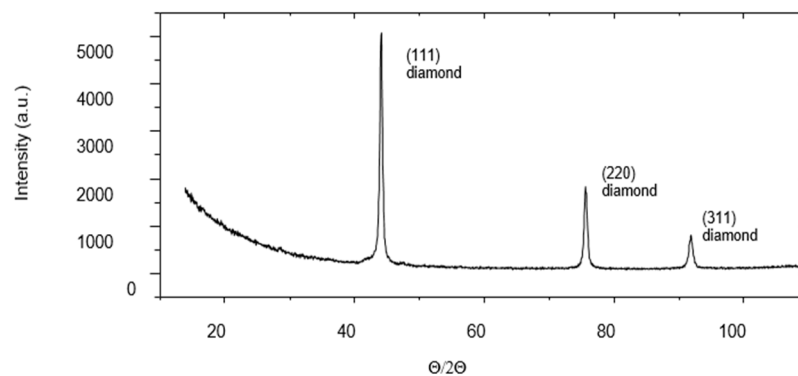
Figure 2. XRD pattern measured on the as-deposited Al_2O_3 /NCD film.

Figure 3 shows COF vs number of cycles curves. The behavior of the NCD and Al_2O_3/NCD films strongly differs for the tests at RT (Figure 3a). The COF value for Al_2O_3/NCD films is high (0.6–0.8), due to contact between the alumina layer and Si_3N_4 ball. The superlubricating behavior with the COF value between 0.004–0.04 was observed for the tests at 300 °C, independent of the type of the samples, with the smallest COF value corresponding to the Al_2O_3/NCD and A-Al_2O_3/NCD films (Figure 3b). The shape of the curves was similar as well. Noticeably different frictional behavior was observed for the tests at 450 °C (Figure 3c). In the case of NCD film, after a relatively long run-in period with the COF value decreasing from 0.8 to 0.5, the COF drops to 0.1 and steadily increases to 0.23 and stabilizes for 15,000 cycles long, after that it increases again to about 0.33 and stabilizes. Similar frictional behavior was found on the NCD films grown on WC-Co and tested at 450 °C [5]. However, the COF curves with shorter run-in and the COF value for the steady sliding period between 0.13–0.17 were found for the Al_2O_3/NCD and A-Al_2O_3/NCD films. Figure 4 shows the morphology of the wear scar surfaces for the NCD and Al_2O_3/NCD films after the tests at 300 °C and 450 °C; the areas with a polished surface alternate with native surfaces of the NCD films. The islands of the native surface are preserved at the end of the sliding test predominantly on the places of scratches made during seeding of the Si wafer. Wear scars surface after the tests at 450 °C is smoother after 300 °C, indicating more intensive surface polishing at a high temperature. Figure 5 shows the wear scar surface after the test at RT on the Al_2O_3/NCD sample; the images show an alternation of morphology from the center to the outer part of the wear scar.
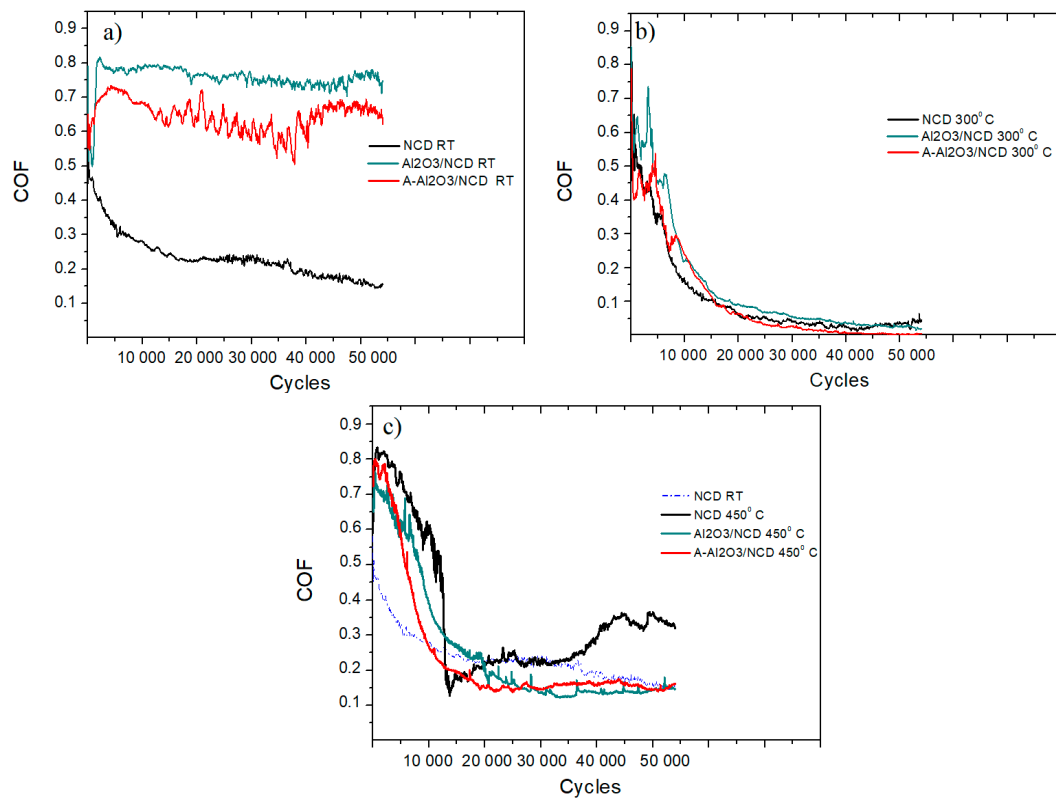
Figure 3. COF vs number of cycle curves taken on the NCD, Al_2O_3/NCD and A-Al_2O_3/NCD films at (**a**) RT, (**b**) 300 °C and (**c**) 450 °C.

The NCD film surface can be seen in the center of the wear scar in Figure 5a (compare with Figure 1a). The oxide islands (Figure 5b) and rubbed surface of alumina (Figure 5c,d) can be seen. Therefore, the high COF value observed for Al_2O_3/NCD and A-Al_2O_3/NCD samples (Figure 3a) for the later stage of sliding at RT can be attributed to contact between the ball and alumina layer, which survived on the borders of the wear scar (Figure 5c,d). The deflection of the NCD film can lead to a loss of contact between the ball and the central part of the wear scar [13,17].

The width of the wear scar observed on the NCD film increases for the test at 450 °C (Figure 6a) in comparison with the tests at RT and 300 °C. The sliding test duration was 3 h and the preheating period took 2 h to heat the sample up to 450 °C. Therefore, the entire surface of the NCD film was exposed to air at high temperature during the experiment, thus the NCD film surface was oxidized and the crystal structure of the top layer of the film was changed. It can result in the enlargement of the wear scar width. In contrast, no such effect was found on the Al_2O_3/NCD and A-Al_2O_3/NCD films at the same temperature (Figure 6b,c). Thus, for these samples, due to protection by the alumina layer, the properties of the NCD films were preserved. The enlargement of the wear scar for the NCD film tested at 450 °C occurs probably after 35,000 cycles of sliding (Figure 3c), because during the 20,000–35,000 cycles period, the COF value for the NCD films tested at RT and 450 °C is the same. In the case of Al_2O_3/NCD and A-Al_2O_3/NCD films, a decrease of the wear scar width for the tests at 450 °C in contrast to ones at RT and 300 °C can be observed. However, the depth of the wear scars is higher after the tests at 450 °C for all types of samples, which can be explained by the increase of the wear as well as by surface deflection [13,17].
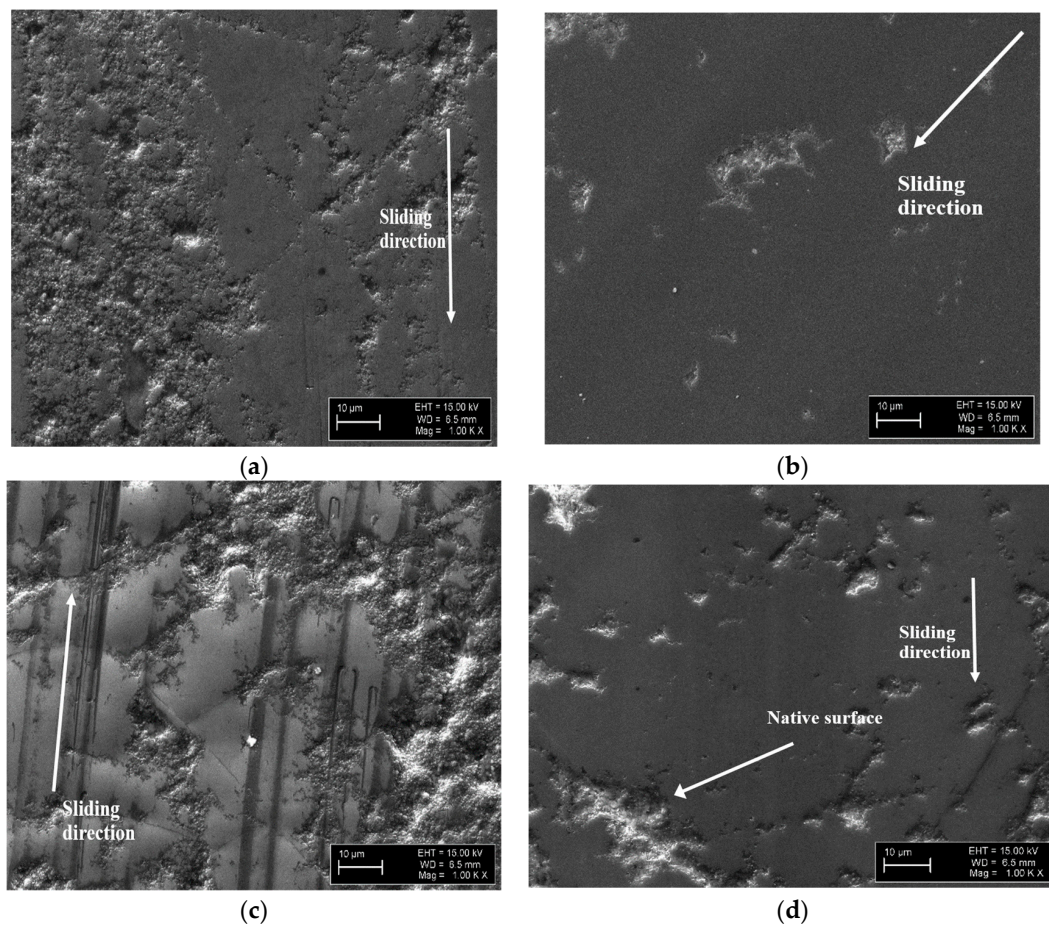
Figure 4. Surface morphology of the wear scars after the tests on the NCD film at (**a**) 300 °C and (**b**) 450 °C, and on the Al$_2$O$_3$/NCD film at (**c**) 300 °C and (**d**) 450 °C.
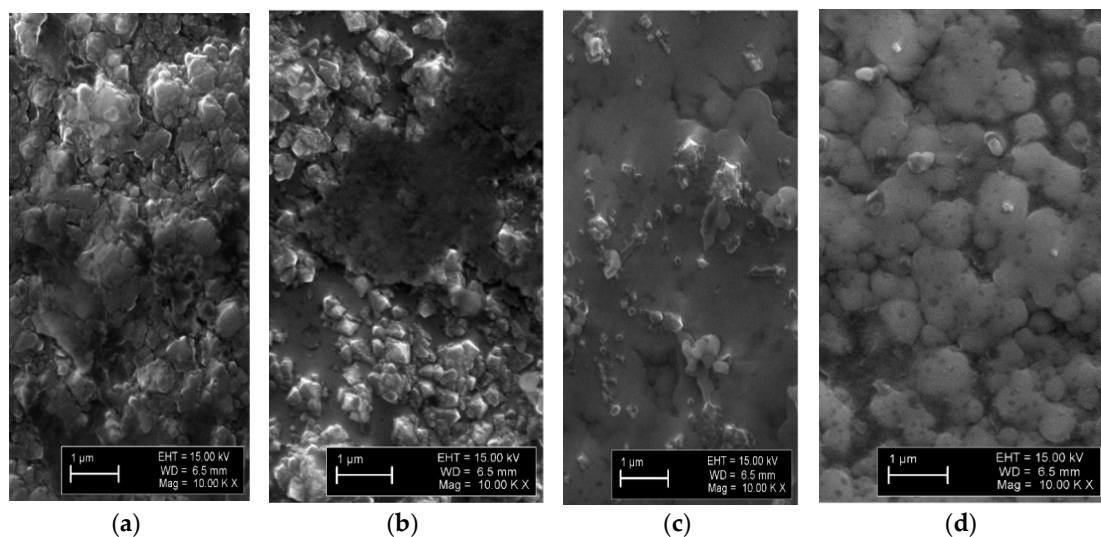
Figure 5. SEM images taken on the wear scar after the test at RT on the Al$_2$O$_3$/NCD film. The images were taken from (**a**) the center of the wear scar (**b**,**c**) were taken in the middle of the wear scar to (**d**) the border of the wear scar images.

The results shown in Figure 7 confirm a significant increase of the wear scar width after the test at 450 °C on the NCD film (Figure 6a). The size of the worn surface on the ball increases correspondingly,

see Figure 8. The size of the worn surface on the balls after the test at RT on the Al_2O_3/NCD and A-Al_2O_3/NCD films is larger in comparison with the tests at 300 and 400 °C, due to higher COF and wear between the Si_3N_4 ball and alumina layer. However, the worn surface is very smooth.
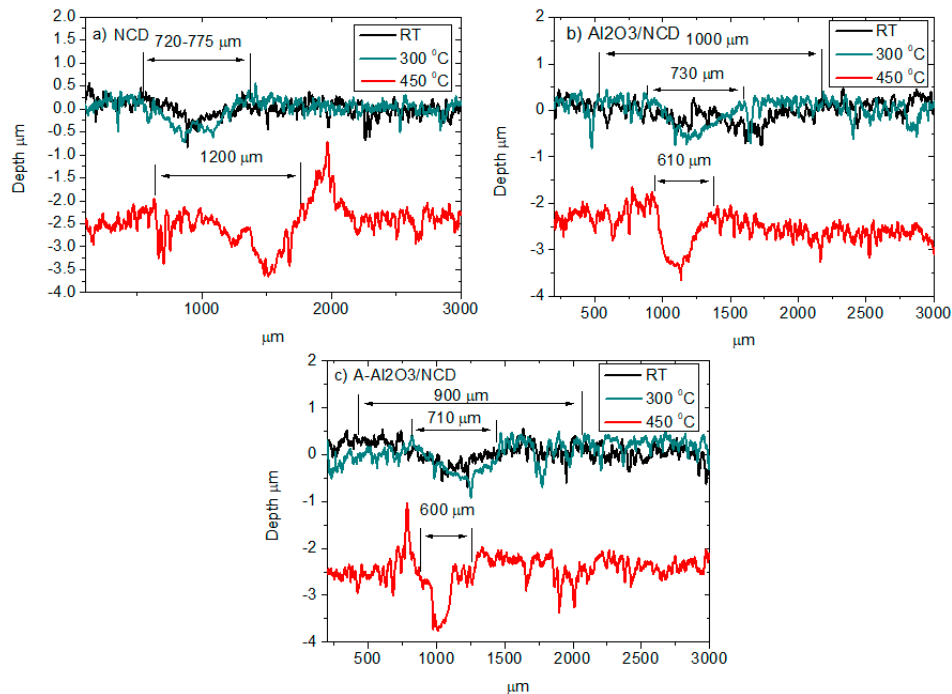
Figure 6. Line scans across the wear scars taken on the (**a**) NCD, (**b**) Al_2O_3/NCD and (**c**) A-Al_2O_3/NCD films.
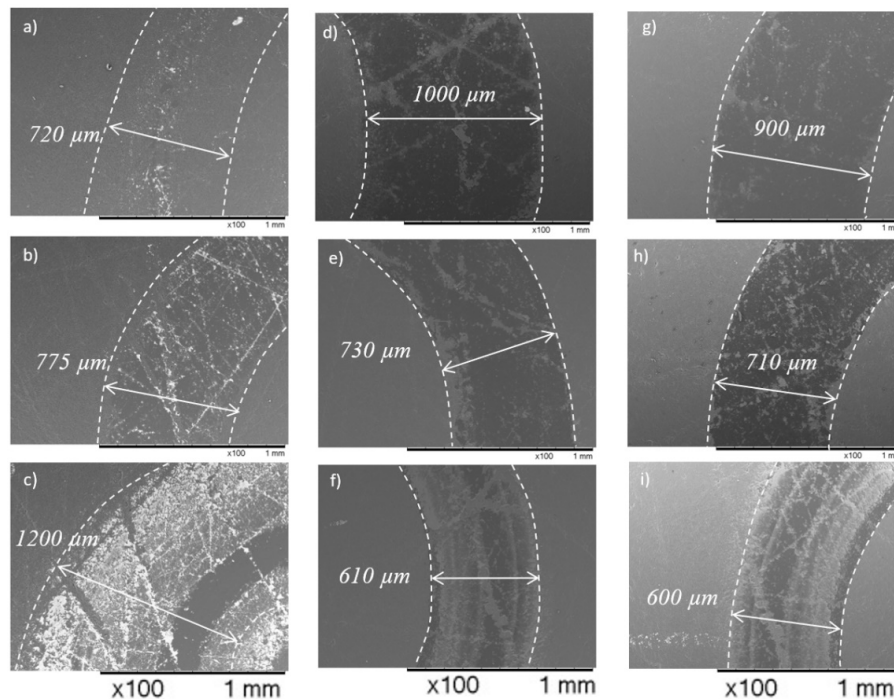
Figure 7. SEM images of the wear scars after sliding tests on the NCD film at (**a**) RT, (**b**) 300 °C and (**c**) 450 °C; Al_2O_3 /NCD film at (**d**) RT, (**e**) 300 °C and (**f**) 450 °C; and A-Al_2O_3 /NCD film at (**g**) RT, (**h**) 300 °C and (**i**) 450 °C.
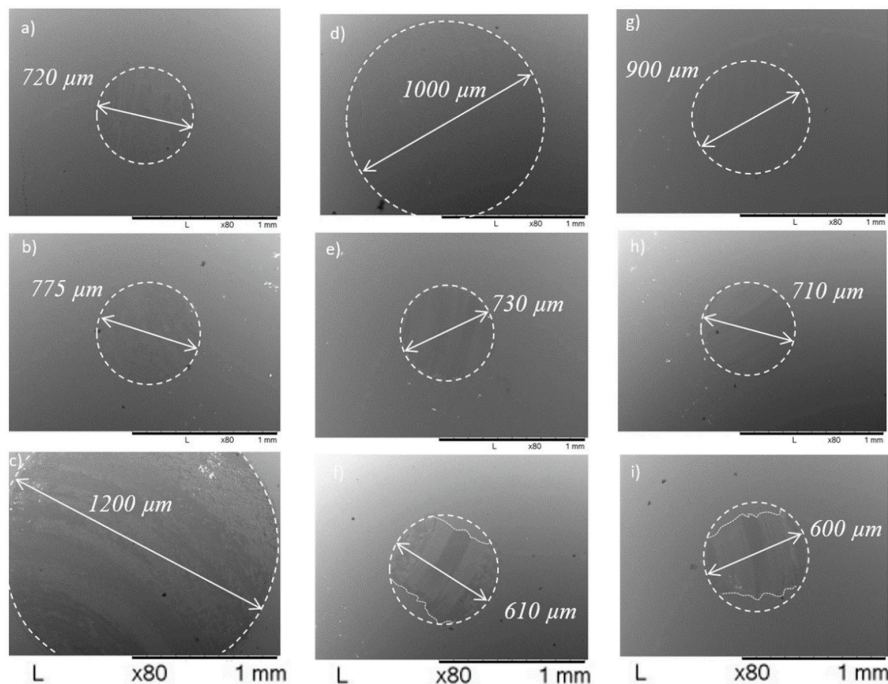
Figure 8. SEM images of the worn surface on the balls after sliding tests against the NCD film at (**a**) RT, (**b**) 300 °C and (**d**) 450 °C; Al$_2$O$_3$ /NCD film at (**d**) RT, (**e**) 300 °C and (**f**) 450 °C; and A-Al$_2$O$_3$ /NCD film at (**g**) RT, (**h**) 300 °C and (**i**) 450 °C.

The measurement of the apparent wear volume on the films is in agreement with the previous results, i.e., the highest wear was observed on the NCD film after the test at 450 °C (Figure 9).

Raman spectra (Figure 10) taken on the native surface of the NCD and Al$_2$O$_3$/NCD films after the tests at different temperatures are similar to ones investigated in our previous studies of the NCD films [5,12,13]. The main peak positions are as follows: 1336 cm^{-1} (diamond), 1366 cm^{-1} (D band), 1549 cm^{-1} (G band), 1135 cm^{-1}, and 1480 cm^{-1} (t-Pa, trans-polyacetylene). No phase transitions or formation of the new compounds due to deposition of alumina can be stated (Figure 10b) in agreement with XRD measurements (Figure 2) and Ref. [10]. There are no clear differences in spectra between different types of samples and temperature of the tests, in spite of diverse data obtained from tribological tests. Raman spectroscopy is a bulk sensitive method, therefore, it could indicate that the properties of a top surface could play an important role to explain friction and wear of the investigated specimens.
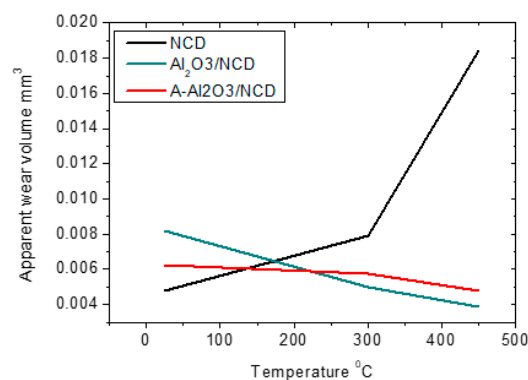
Figure 9. Apparent wear volumes of the wear scars measured on the NCD, Al$_2$O$_3$/NCD and A-Al$_2$O$_3$/NCD films.
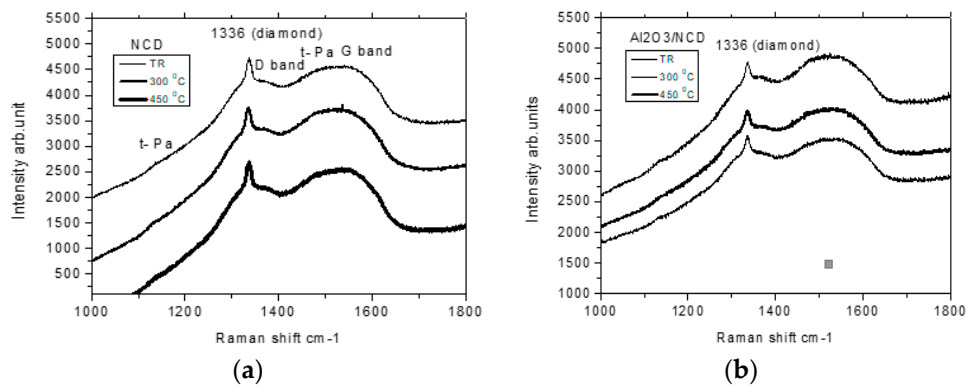
Figure 10. Raman spectra taken on the (**a**) NCD and (**b**) Al_2O_3/NCD films.

Figures 11–14 shows the XPS spectra of O 1s, C 1s, and Si 2p peaks. The position of the O 1s peak in spectra taken on the pristine surface of NCD and Al_2O_3/NCD films differs due to different chemical bonding of oxygen within an alumina layer and oxygen absorbed on the NCD film surface from air (Figure 11). The O 1s peak in spectra taken on the NCD film locates at 532.4 eV, however, it is shifted to 531.4 eV for the Al_2O_3/NCD film. The position of the peak at 531.4 eV was found on the alumina film surfaces elsewhere [18], therefore, the formation of the alumina layer on top of the NCD film is confirmed. In contrast, there is a similarity in spectra taken within the wear scars after the tests at RT between both types of samples (NCD and Al_2O_3/NCD), i.e., the O 1s peak position is 532.8-533 eV. The measurement was carried out in the central part of the wear scar on the Al_2O_3/NCD film (Figure 5a). There is a similarity between the O 1s peak positions (532.4-532.5 eV) in spectra taken within the wear scars on both samples after the tests at 300 °C as well. In other words, similar chemical reactions occur during sliding independent of types of samples at RT and 300 °C. In the case of spectra taken within the wear scars after the tests at 450 °C, similar peaks at 532.2-532.5 eV can be seen for both types of samples. However, a peak at 534.6 eV can be observed only for the NCD film, indicating a difference in chemical kinetics on the NCD and Al_2O_3/NCD films during sliding at 450 °C.
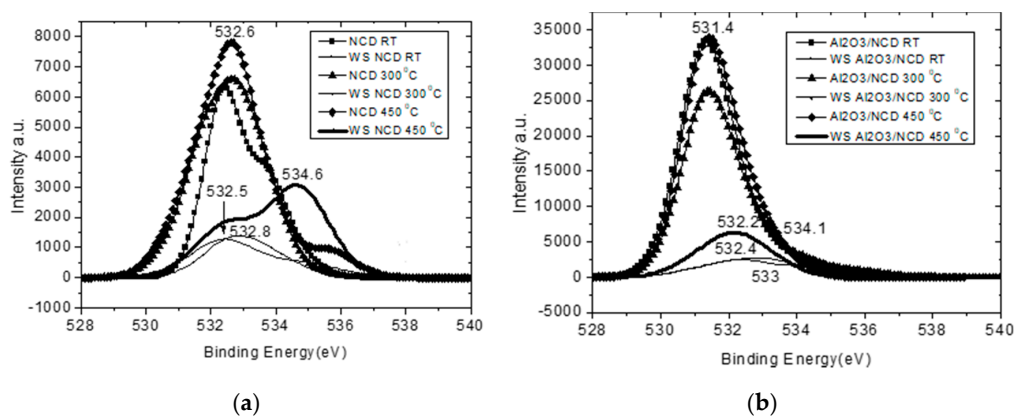
Figure 11. XPS spectra of the O 1s peak (WS-wear scar) taken on the (**a**) NCD and (**b**) Al_2O_3/NCD films.

In the case of XPS spectra taken on the native NCD surface, the C 1s peak position is 284.4 eV for the samples investigated at RT and 300 °C (Figure 12a). However, the C 1s peak is shifted to a higher value 285.7 eV for the NCD film heated up to 450 °C (Figures 12a and 13b), indicating alteration of the chemical composition on top of the NCD film after heating at elevated temperature. The deconvolution of the spectrum revealed that the peak at 285.7 eV corresponds to sp^3 bonding (Figure 13b). Due to heating at 450 °C, the sp^2 bonds were likely oxidized and desorbed from the surface as carbon-based gases [2,3], which finally led to the sp^3 enrichment of the NCD film surface. In contrast, the NCD surface at RT is sp^2 enriched (Figure 13a), as well as after heating up to 300 °C (not shown). It is

worth stressing, that upon oxidation, the C 1s peak moves to a higher value as well [19], therefore, the observed results indicate an oxidation of the NCD film surface at 450 °C. In addition, Larsson et al. [1] reported that a significant increase of diamond surface hydrophilicity was observed at 450 °C. Therefore, the C 1s peak position after the heating of the clean NCD surface at 450 °C in ambient air can indicate the sp^3-enriched surface as well as oxidation of the surface. In conclusion, we believe that sp^3 surface enrichment occurs due to higher surface hydrophilicity, resulting in extensive etching of the sp^2 bonds on the NCD film surface. After sliding tests at RT and 300 °C, the position of C 1s peak at 284.9 eV corresponds to the oxidized surface of the NCD film within the wear scar (Figure 12a), the same position of the C 1s peak (285 eV) was found for the Al_2O_3/NCD films (Figure 12b). The C 1s peak position at 285 eV was reported for the native NCD surface upon oxidation [19]. Finally, after the tests at 450 °C, the C 1s peak positions for the NCD and Al_2O_3/NCD films were different, i.e., at 285.2 and 284.6 eV, respectively (Figure 12a,b).

Figure 14 shows XPS spectra of the Si 2p peaks. The peak at 102.8-103 eV corresponds to SiO_2 [20], which possesses good lubricating properties [21]. In the course of sliding, the wear of the Si_3N_4 ball takes place, which results in formation of SiO_2 within the wear scar. After the wear tests at RT, the peak positions were slightly different, i.e., at 102.9 and 103.7 eV for the NCD and Al_2O_3/NCD films, respectively. There is a similarity between XPS spectra taken after the tests at 300 °C on both samples, namely two peaks at 103-103.4 and 105-105.5 eV can be observed in the spectra. It indicates similar chemical kinetics during sliding at 300 °C. However, after the tests at 450 °C, the peak positions differ significantly, i.e., at 105.1 and 102.8 eV for the NCD and Al_2O_3/NCD films, respectively.
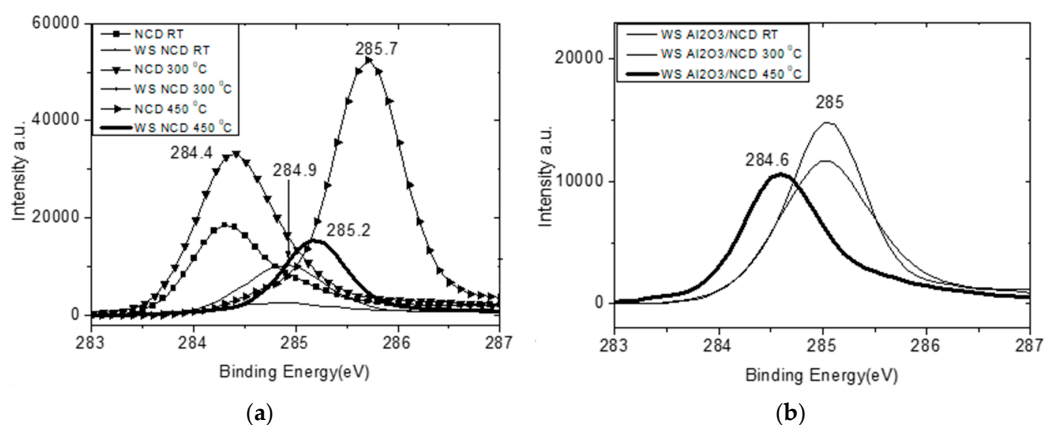
Figure 12. XPS spectra of the C 1s peak taken on the (**a**) NCD and (**b**) Al_2O_3/NCD films.
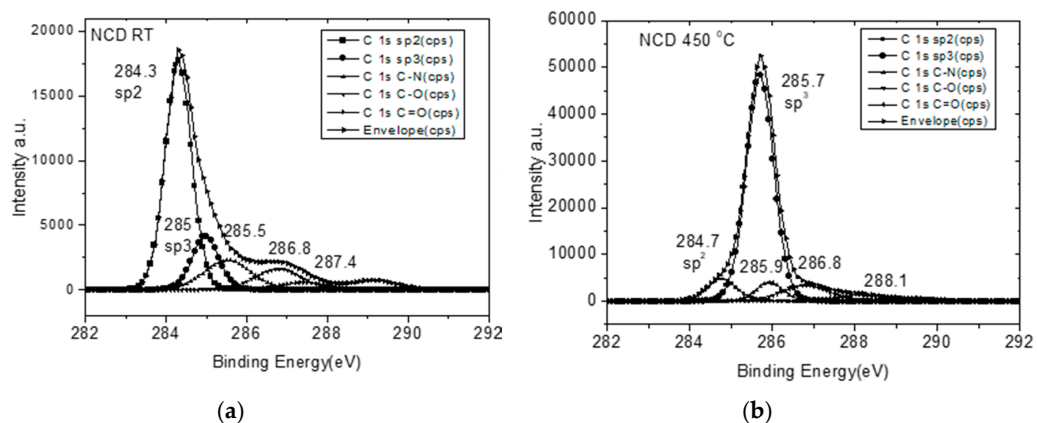
Figure 13. XPS spectra of the C 1s peak taken on the NCD film native surface at (**a**) RT and after the heating at (**b**) 450 °C.

(a)

(b)
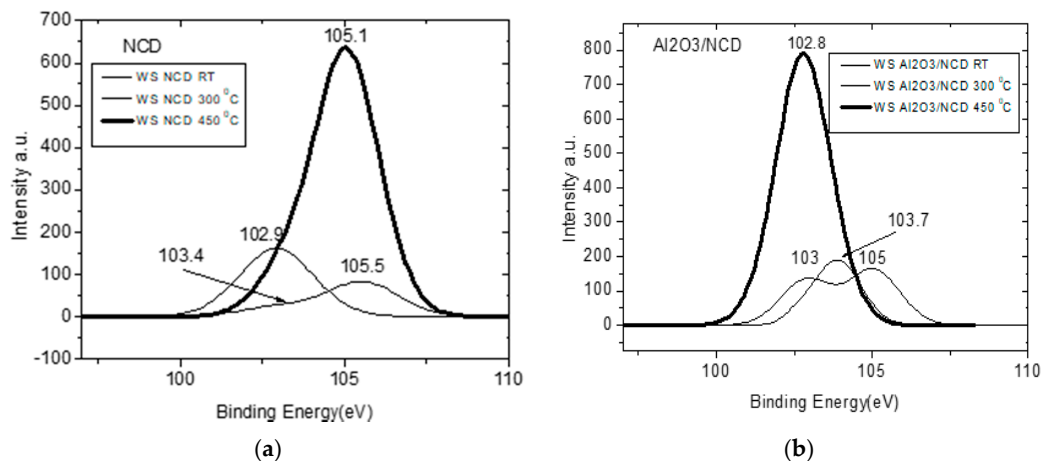
Figure 14. XPS spectra of the Si 2p peak taken on the (**a**) NCD and (**b**) Al_2O_3/NCD films.

The Raman and XPS spectra taken on the A-Al_2O_3/NCD films (not shown) were similar to ones on the Al_2O_3/NCD films.

To summarize the discussion on the XPS data obtained from investigation of the wear scar surfaces in the case of tests at RT, the O 1s and C 1s peaks positions are very similar for the NCD and Al_2O_3/NCD films. However, there is a shift between the Si 2p peak positions. The COF value for RT tests differs for the NCD and Al_2O_3/NCD films (Figure 3), due to specific wear mechanisms on the Al_2O_3/NCD films explained above, which cannot be related with XPS analysis. In the case of tests at 300 °C, XPS spectra of any elements (O, C and Si) measured within the wear scars are very similar independent of the type of samples. The ultra-low COF value (0.004-0.04) and relatively low wear were found in tests at 300 °C on both types of samples (Figures 3 and 9), which could indicate similar tribological conditions within the contact. Therefore, the XPS analysis confirms the similarity in friction and wear behavior observed in tribological tests at 300 °C. The onset of superlubricity can be attributed to the changes within the carbonaceous and surface passivation layers at elevated temperature [1,4,21–23]. The spectra of the same elements (O, C and Si) taken after the tests at 450 °C show clear differences between the two types of samples, supporting an observed difference in tribological behavior. The COF behavior found at the final stage of the sliding test at 450 °C on the Al_2O_3/NCD film is similar to the COF found for the NCD film in the test at RT (Figure 3), as well as the wear on both specimens was similar (Figure 9). It could indicate similar tribological conditions in these tests taken at different temperatures. It is interesting to note that the position of the C 1s peak in the spectrum taken within the wear scar on the Al_2O_3/NCD film after the test at 450 °C (Figure 12b) is similar to the position of the peak observed on the native NCD surface at RT (Figure 12a). Finally, the A-Al_2O_3/NCD films annealed at 500 °C in air show improved tribological behavior in contrast to the uncoated NCD ones (Figures 3 and 9). Therefore, a protection of the entire film surface against oxygen attack at 450-500 °C and an effect of preservation of the superior properties of diamond films at 300 and 450 °C in air by deposition of a thin alumina layer is demonstrated. The oxidation retardation at high temperature by formation of a thin B_2O_3 layer on a boron-doped diamond surface is another example of the formation of a protective oxide layer on the diamond films [2].

The increase of the wear scar width on the NCD film and the size of the worn surface on the Si_3N_4 ball after the test at 450 °C is worth comparing with the tests on the diamond films deposited on SiC substrate and tested against SiC pin at 400 °C [4]. The Raman spectra taken on the diamond films in Refs. [4,5] are similar to the one measured in the present study, i.e., the structure of the diamond films is similar. A significant increase of the SiC pin wear reported in Ref. [4] means an increase in size of the worn surface on the pin and wear scar width on the film as well, which is in a good agreement with the results obtained at 450 °C in the present study and Ref. [5]. Therefore, the intensive degradation of the diamond film surface in tribological tests could start already at 400 °C. The sp^3 surface enrichment

of the NCD film was observed at 450 °C in the present study, which indicates sp^2 bonding etching and diamond film surface modification. The temperature of 400 °C reported in Ref. [4] is lower than this temperature probably due to the intensive heating produced during sliding. The severe wear of diamond film can be facilitated rather on the border of the wear scar where the damaged layer of the diamond film is continuously formed due to high temperature and exposure to ambient air, which results in accelerated widening of the wear scar. In general, the onset of the degradation can likely depend on the type of the diamond film and tribological test conditions.

4. Conclusions

To protect the NCD film against oxidation attack at high temperature in ambient air, the thin alumina layer was deposited on top of the NCD film. The superlubricating behavior was observed in sliding tests at 300 °C with the COF value between 0.004-0.04 for all types of samples, i.e., NCD, Al_2O_3/NCD and A-Al_2O_3/NCD films. It indicates that the thin alumina layer does not deteriorate the properties of the NCD films at low temperature. This finding was confirmed by means of the XPS investigations, which revealed similar chemical composition within the wear scars for all samples. In the case of the tests at RT, the XPS spectra taken within the central part of the wear scars also showed rather similar chemical composition when uncoated and coated with alumina NCD films. However, the COF value for the steady state period of sliding at RT was different between the NCD and Al_2O_3/NCD specimens, due to the fact that friction was affected by the contact between the alumina layer on the border of the wear scars and the ball. On the other hand, the protection of the entire surface of the NCD films by alumina layer against oxidation and preservation of the excellent properties of diamond films were shown in the wear tests at 450 °C.

References

1. Larsson, K.; Björkman, H.; Hjort, K. Role of water and oxygen in wet and dry oxidation of diamond. *J. Appl. Phys.* **2001**, *90*, 1026–1034. [CrossRef]
2. Herrmann, M.; Matthey, B.; Gestrich, T. Boron-doped diamond with improved oxidation resistance. *Diam. Relat. Mater.* **2019**, *92*, 47–52. [CrossRef]
3. Pu, J.-C.; Wang, S.-F.; Sung, J.C. High-temperature oxidation behavior of nanocrystalline diamond films. *J. Alloys Compd.* **2010**, *489*, 638–644. [CrossRef]
4. Erdemir, A.; Fenske, G.R. Tribological performance of diamond and diamond like carbon films at elevated temperatures. *Tribol. Trans.* **1996**, *39*, 787–794. [CrossRef]
5. Yashin, M.; Baronins, J.; Menezes, P.L.; Viljus, M.; Raadik, T.; Bogatov, A.; Antonov, M.; Podgursky, V. Wear rate of nanocrystalline diamond coating under high temperature sliding conditions. *Solid State Phenom.* **2017**, *267*, 219–223. [CrossRef]
6. Abou Gharam, A.; Lukitsch, M.J.; Balogh, M.P.; Irish, N.; Alpas, A.T. High temperature tribological behavior of W-DLC against aluminum. *Surf. Coat. Technol.* **2011**, *206*, 1905–1912. [CrossRef]
7. Choi, J.; Nakao, S.; Ikeyama, M.; Kato, T. Effect of oxygen plasma treatment on the tribological properties of Si-DLC coatings. *Phys. Stat. Sol. (C)* **2008**, *5*, 956–959. [CrossRef]

8. Yang, B.; Zheng, Y.; Zhang, B.; Wei, L.; Zhang, J. The high-temperature tribological properties of Si-DLC films. *Surf. Interface Anal.* **2012**, *44*, 1601–1605. [CrossRef]

9. Dominguez, D.; Tiznado, H.; Borbon-Nuñez, H.A.; Muñoz-Muñoz, F.; Romo-Herrera, J.M.; Soto, G. Enhancing the oxidation resistance of diamond powder by the application of Al_2O_3 conformal coat by atomic layer deposition. *Diam. Relat. Mater.* **2016**, *69*, 108–113. [CrossRef]

10. Kawakami, N.; Yokota, Y.; Tachibana, T.; Hayashi, K.; Kobashi, K. Atomic layer deposition of Al_2O_3 thin films on diamond. *Diam. Relat. Mater.* **2005**, *14*, 2015–2018. [CrossRef]

11. Åstrand, M.; Selinder, T.I.; Fietzke, F.; Klostermann, H. PVD-Al_2O_3 -coated cemented carbide cutting tools. *Surf. Coat. Technol.* **2004**, *188–189*, 186–192. [CrossRef]

12. Podgursky, V.; Bogatov, A.; Sedov, V.; Sildos, I.; Mere, A.; Viljus, M.; Buijnsters, J.G.; Ralchenko, V. Growth dynamics of nanocrystalline diamond films produced by microwave plasma enhanced chemical vapor deposition in methane/hydrogen/air mixture: Scaling analysis of surface morphology. *Diam. Relat. Mater.* **2015**, *58*, 172–179. [CrossRef]

13. Podgursky, V.; Bogatov, A.; Yashin, M.; Viljus, M.; Bolshakov, A.P.; Sedov, V.; Volobujeva, O.; Mere, A.; Raadik, T.; Ralchenko, V. A comparative study of the growth dynamics and tribological properties of nanocrystalline diamond films deposited on the (110) single crystal diamond and Si(100) substrates. *Diam. Relat. Mater.* **2019**, *92*, 159–167. [CrossRef]

14. Jõgiaas, T.; Zabels, R.; Tamm, A.; Merisalu, M.; Hussainova, I.; Heikkilä, M.; Mändar, H.; Kukli, K.; Ritala, M.; Leskelä, M. Mechanical properties of aluminum, zirconium, hafnium and tantalumoxides and their nanolaminates grown by atomic layer deposition. *Surf. Coat. Technol.* **2015**, *282*, 36–42. [CrossRef]

15. Homola, T.; Buršíková, V.; Ivanova, T.V.; Souček, P.; Maydannik, P.S.; Cameron, D.; Lackner, C.J.M. Mechanical properties of atomic layer deposited Al_2O_3/ZnO nanolaminates. *Surf. Coat. Technol.* **2015**, *284*, 198–205. [CrossRef]

16. Lee, J.S.; Min, B.; Cho, K.; Kim, S.; Park, J.; Lee, Y.T.; Kim, N.S.; Lee, M.S.; Park, S.O.; Moon, J.T. Al_2O_3 nanotubes and nanorods fabricated by coating and filling of carbon nanotubes with atomic-layer deposition. *J. Cryst. Growth* **2003**, *254*, 443–448. [CrossRef]

17. Podgursky, V.; Bogatov, A.; Sobolev, S.; Viljus, M.; Sedov, V.; Ashkinazi, E.; Ralchenko, V. Effect of nanocrystalline diamond films deflection on wear observed in reciprocating sliding tests. *J. Coat. Sci. Technol.* **2016**, *3*, 109–115. [CrossRef]

18. Reddy, N.; Bera, P.; Reddy, V.R.; Sridhara, N.; Dey, A.; Anandan, C.; Sharma, A.K. XPS study of sputtered alumina thin films. *Ceram. Int.* **2014**, *40*, 11099–11107. [CrossRef]

19. Seshan, V.; Ullien, D.; Castellanos-Gomez, A.; Sachdeva, S.; Murthy, D.H.K.; Savenije, T.J.; Ahmad, H.A.; Nunney, T.S.; Janssens, S.D.; Haenen, K.; et al. Hydrogen termination of CVD diamond films by high-temperature annealing at atmospheric pressure. *J. Chem. Phys.* **2013**, *138*, 234707-1–234707-6. [CrossRef]

20. Li, M.; Zeng, L.; Chen, Y.; Zhuang, L.; Wang, X.; Shen, H. Realization of Colored Multicrystalline Silicon Solar Cells with SiO_2/SiN_x:H Double Layer Antireflection Coatings. *Int. J. Photoenergy* **2013**, *1*, 1–8. [CrossRef]

21. Zeng, Q.; Eryilmaz, O.; Erdemir, A. Superlubricity of the DLC films-related friction system at elevated temperature. *RSC Adv.* **2015**, *5*, 93147–93154. [CrossRef]

22. Ando, T.; Yamamoto, K.; Ishii, M.; Kamo, M.; Sato, Y. Vapour-phase oxidation of diamond surfaces in O_2 studied by diffuse reflectance fourier-transform Infrared and temperature-programmed desorption spectroscopy. *J. Chem. Soc. Faraday Trans.* **1993**, *89*, 3635–3640. [CrossRef]

23. Konicek, A.R.; Grierson, D.S.; Sumant, A.V.; Friedmann, T.A.; Sullivan, J.P.; Gilbert, P.U.P.A.; Sawyer, W.G.; Carpick, R.W. Influence of surface passivation on the friction and wear behavior of ultrananocrystalline diamond and tetrahedral amorphous carbon thin films. *Phys. Rev. B* **2012**, *85*, 155448-1–155448-13. [CrossRef]